The Properties of Matter
in White Dwarfs and Neutron Stars

Shmuel Balberg and Stuart L. Shapiro*

Department of Physics, University of Illinois at Urbana-Champaign,

1110 W. Green St., Urbana, IL 61801

Abstract

White dwarfs and neutron stars are stellar objects with masses comparable to that of our sun. However, as the endpoint stages of stellar evolution, these objects do not sustain any thermonuclear burning and therefore can no longer support the gravitational load of their own mass by generating thermal pressure. Rather, matter in their interiors is compressed to much higher densities than commonly found in normal stars, and pressure is created by degenerate fermion kinetic energy and particle interactions. As a result, white dwarfs and neutron stars offer unique cosmic laboratories for studying matter at very high densities. In this review we discuss the basic properties of condensed matter at extreme densities and summarize the extent to which these properties can be examined by observations of compact objects.

I.   Introduction

Astronomical phenomena provide many examples where matter exists in extreme conditions not found in terrestrial environments. One example is the high density of degenerate matter in "compact objects" - the relics of stars that have ceased burning thermonuclear fuel, and thereby no longer generate thermal pressure to support themselves against gravitational collapse. By contracting appreciably from their original sizes, the interiors of compact objects reach sufficiently high densities to produce nonthermal pressure via degenerate fermion pressure and particle interactions. Compact objects provide cosmic laboratories for studying the properties of matter at high densities.

Firm observational evidence and well-founded theoretical understanding both exist for two classes of compact objects which support themselves against collapse by cold, degenerate fermion pressure: **white dwarfs**, whose interiors resemble a very dense solid, with an ion lattice surrounded by degenerate electrons, and **neutron stars**, whose cores resemble a giant atomic nucleus - a mixture of interacting nucleons and electrons, and possibly other elementary particles and condensates. White dwarfs are supported by the pressure of degenerate electrons, while neutron stars

---

*also Department of Astronomy and National Center for Supercomputing Applicaions, University of Illinois at Urbana-Champaign, Urbana, IL 61801

are supported by pressure due to a combination of nucleon degeneracy and nuclear interactions. These unique states of matter are achieved by significant compression of stellar material. Table 1 compares the principal physical quantities of a typical white dwarf and neutron star with those of the sun[1].

Table 1: Parameters for the sun and a typical white dwarf and neutron star.

object	mass $(M_\odot$ [a]$)$	radius (km)	mean density (gm cm^{-3})	mean pressure (dyne cm^{-2})	GM/Rc^2 [b]
Sun	1	$\sim 7 \times 10^5$	~ 1	$\sim 10^{12}$	$\sim 10^{-6}$
White Dwarf	≤ 1.4	$\sim 5 \times 10^3$	$\sim 10^7$	$\sim 10^{24}$	$\sim 10^{-4}$
Neutron Star	1-3	~ 10	$\sim 10^{14}$	$\sim 10^{34}$	$\sim 10^{-1}$

[a] - $M_\odot \equiv 1.989 \times 10^{33}$ gm $=$ one solar mass.
[b] - This ratio measures the importance of relativistic gravitation, i.e., general relativity.

Condensed matter in compact objects spans an enormous range of densities, which we loosely refer to as "high densities". These extend from about $7\,\mathrm{gm\,cm^{-3}}$ (e.g., the density of terrestrial $^{56}_{26}$Fe), at the surface of a cold neutron star or white dwarf, to as much as $\rho \approx 10^{15}\,\mathrm{gm\,cm^{-3}}$, several times the density in atomic nuclei, in the cores of neutron stars. Matter at the various densities found in compact objects exhibits a variety of novel properties. Electromagnetic, strong, and weak interactions all play an important role in determining the character of compact objects. Since these objects are bound by gravity, they are a meeting point of all four of the fundamental forces of nature. Correspondingly, the astrophysics of white dwarfs and neutron stars incorporates a wide variety of physics including nuclear, particle, solid state and gravitation physics, to name a few areas.

In this review we briefly survey the theory of condensed matter at high densities in compact objects and illustrate how the basic theory is tested through astronomical observations. Since we must cover fifteen orders of magnitude in density, our presentation is at most introductory in nature, and we encourage the interested reader to pursue the cited references. A detailed introduction to the physics of high density matter and compact objects can be found in the textbook *Black Holes, White Dwarfs and Neutron Stars: the Physics of Compact Objects*, by Shapiro and Teukolsky [1].

We begin by considering the fundamental nature of cold $(T = 0)$ high density matter in Section II., and distinguish between different regimes of high density. In Section III. we connect these microscopic properties with the fundamental macroscopic parameters of a compact object through the hydrostatic equilibrium dependence of mass and radius on central density. We summarize the fundamental predictions regarding the structure of white dwarfs and neutron stars. In Section IV.-V. we examine how observations of white dwarfs and neutron stars can be used to probe the properties high density matter. We briefly discuss the perturbative effects of a finite temperature in Section VI..

---

[1]Throughout this review we will be using units which are the standard in astrophysical research: cgs for microscopic properties of matter and solar units (denoted by $\odot$) for macroscopic properties of astronomical objects.

II. The Cold, High Density Equation of State

The pressure and energies in white dwarfs and neutron stars are nonthermal; thermal effects due to a finite-temperature can be treated as a perturbation. We may therefore treat high density matter as having a zero temperature to very good approximation. The equation of state (EoS) of the matter then reduces to a single-parameter function, $P(\rho_0)$ and $\rho(\rho_0)$, or $P(\rho)$, where P is the pressure, ρ_0 is the rest-mass density and ρ is the total mass-energy density which accounts for internal (possibly relativistic) particle energies as well as rest-mass energy.

There exist two main regimes of high density, distinguished as follows. As long as all nucleons are confined to nuclei, their contribution to the total pressure is negligible compared to that of the degenerate electrons. At some threshold density, ρ_{n-drip}, it becomes favorable for the nuclei to disintegrate, i.e., neutrons "drip" out of the nuclei and form a "nucleon gas". The standard EoS of Baym, Pethick and Sutherland [2] suggests that $\rho_{n-drip} \approx 4 \times 10^{11}$ gm cm^{-3} . We may distinguish between the EoS for $\rho \leq \rho_{n-drip}$ which characterizes matter in white dwarfs and in the outermost layers of neutron stars, and $\rho > \rho_{n-drip}$, which describes matter in the interior of neutron stars.

A. The Equation of State below Neutron Drip Density: $\rho \lesssim 4 \times 10^{11}$ gm cm^{-3}

In matter below the neutron drip density the ions provide a Coulomb lattice of point-like charges, which is (to good approximation) independent of the properties of the surrounding electrons. The EoS of such matter is governed mainly by the electron gas. To lowest approximation, we may treat the electrons as an ideal fermion gas, incorporating some Coulomb corrections at relatively low density ($\rho \leq 10^4$ gm cm^{-3}) and corrections due to inverse $\beta-$decay just below the neutron drip density (10^9 gm cm$^{-3} \leq \rho \leq \rho_{n-drip}$). The EoS of condensed matter below neutron drip density is well understood. The standard equations for cold, degenerate matter in white dwarfs (helium, carbon, oxygen and, possibly iron dominated models) have been derived by Chandrasekar [3] and Salpeter [4], whereas models for equilibrated matter[2], are based on the works of Dirac [5] and Feynman, Metropolis and Teller [6] for $\rho \leq 10^4$ gm cm^{-3} , and e.g., of Harrison and Wheeler [7] and Baym, Pethick and Sutherland [2] for higher densities.

1. The Ideal Fermion Gas

For almost the entire range of high densities the electrostatic energy associated with the structure of matter is much smaller than the Fermi energies. Consequently, Coulomb forces are generally negligible in a first order treatment of the high density EoS. The electron component of high density matter can therefore be described by a cold, single species gas of noninteracting fermions. At zero temperature the fermions fill all the states with momentum $p \leq p_F$ and none of the states with $p > p_F$, where p_F is the Fermi momentum. The corresponding Fermi energy of the particle species

---

[2]The equilibrium isotope of matter is the nucleus of highest binding energy per nucleon. At low densities this isotope is normal $^{56}_{26}$Fe, but as density increases so do the atomic mass and neutron to proton ratio [1].

is

$$E_F \equiv \left((p_F c)^2 + (mc^2)^2\right)^{1/2} , \tag{1}$$

where $c = 3 \times 10^{10}$ cm sec^{-1} is the speed of light in vacuum and m is the fermion rest mass.

For electrons, their number density, n_e, is directly related to their Fermi momentum, $p_{F,e}$ by integrating over all occupied phase space ($h = 6.63 \times 10^{-27}$ ergs sec is Plank's constant):

$$n_e = \int_0^{p_{F,e}} n_e(p) dp \equiv 2\frac{1}{h^3} \int_0^{p_{F,e}} 4\pi p^2 dp = \frac{8\pi p_{F,e}^3}{3h^3} . \tag{2}$$

The factor of 2 in the second equation arises from the electron spin degeneracy.

The pressure the electrons supply is calculated through the mean momentum flux of the electron gas,

$$P = \frac{1}{3} \int_0^{p_{F,e}} v_e(p) n_e(p) p dp = \frac{2}{h^3} \int_0^{p_{F,e}} \frac{p^2 c^2}{(p^2 c^2 + (mc^2)^2)^{1/2}} 4\pi p^2 dp = \frac{m_e c^2}{\lambda_e^3} \phi(x) , \tag{3}$$

where $x_e \equiv p_{F,e}/m_e c$ is the electron "relativity parameter", $\lambda_e \equiv h/(2\pi m_e c)$ is the electron Compton wavelength, $v_e = p_e c^2/E_e$ is the electron velocity and

$$\phi(x) = \frac{1}{8\pi^2} \left\{ x(1+x^2)^{1/2}(2x^2/3 - 1) + \ln\left[x + (1+x^2)^{1/2}\right] \right\} . \tag{4}$$

The mass-energy density of the free electrons is also uniquely related to the Fermi momentum as

$$\varepsilon_e = \int_0^{p_{F,e}} E_e(p) n_e(p) dp = \frac{2}{h^3} \int_0^{p_{F,e}} (p^2 c^2 + (mc^2)^2)^{1/2} 4\pi p^2 dp = \frac{mc^2}{\lambda_e^3} \chi(x_e) ; \tag{5}$$

where

$$\chi(x) = \frac{1}{8\pi^2} \left\{ x(1+x^2)^{1/2}(1+2x^2) - \ln\left[x + (1+x^2)^{1/2}\right] \right\} . \tag{6}$$

However, even when the degenerate electrons contribute most of the pressure, the mass-energy density is dominated by the rest mass of the ions, which are very nonrelativistic at these densities. Thus, the density of the matter may be simply taken as

$$\rho = \rho_0 = \frac{n_e m_B}{Y_e} , \tag{7}$$

where Y_e is the mean number of electrons per nucleon and m_B is the mean nucleon mass. In the case of white dwarfs we may set $Y_e = Z/A = 0.5$ (Z =atomic number, A =atomic weight) which is appropriate for fully ionized helium, carbon or oxygen, the most abundant constituents in a white dwarf, and $m_B = 1.66 \times 10^{-24}$ gm. Combining Eqs. (2), (3) and (7) provides the basic EoS of electron-pressure dominated high-density condensed matter in this regime.

There exist opposite limits to the cold fermion gas equation of state: the low density, nonrelativistic ($x \ll 1$) and the high density, extremely relativistic ($x \gg 1$) limits. From Eqs. (2) and (7) we find that in cold matter with $Y_e = 0.5$ the electron relativity parameter satisfies $x_e = 1$ at $\rho \approx 10^6$ gm cm^{-3} , which therefore marks the transition density between a nonrelativistic (NR)

4

and extremely relativistic (ER) electron gas. It is convenient to write the EoS in the two limits in a *polytropic* form,

$$P(\rho) = K\rho^{\Gamma} \tag{8}$$

where

$$\text{NR} \quad x_e \ll 1, \; \rho \ll 10^6 \text{gm cm}^{-3} \; : \; \Gamma = \frac{5}{3}, \; K = 1.0036 \times 10^{13} Y_e^{5/3} \; ; \tag{9}$$

$$\text{ER} \quad x_e \gg 1, \; \rho \gg 10^6 \text{gm cm}^{-3} \; : \; \Gamma = \frac{4}{3}, \; K = 1.2435 \times 10^{15} Y_e^{4/3} \; . \tag{10}$$

The constant K is in cgs units, yielding a pressure in dyne cm^{-2} for a density in gm cm^{-3} . Note that in this approximation the composition of the matter enters only through Y_e. Correspondingly, helium, carbon and oxygen, which all have $Y_e = 0.5$ have identical ideal equations of state, slightly stiffer than that of iron ($Y_e = 26/56 \approx 0.43$). Fully equilibrated matter (often referred to as "catalyzed") has a Y_e that decreases with density and is therefore softer than matter composed of a single element.

The free, degenerate electron pressure EoS outlined here is a good approximation for the equation of state below neutron-drip density. It was employed by Chandrasekar in his pioneering analysis of equilibrium white dwarfs [3], for which he received the Nobel prize in 1983. More exact treatments were introduced in later years, which included the two main required corrections - electrostatic effects at low densities, and neutronization (or inverse $\beta-$decay) at higher densities.

2.   Electrostatic Corrections to the Cold Equation of State: $\rho \lesssim 10^4$ gm cm^{-3}

There exists a net electrostatic correction to the ideal equation of state due to the fact that the local distribution of charge is very nonuniform. The fact that positive charge is concentrated in point-like ions causes the average electron-ion separation to be smaller than the average distance between electrons. The net electrostatic potential felt by the electrons is thus an attractive one, which effectively reduces the pressure for a given density.

Electrostatic corrections to the cold equation state are mostly important at relatively low densities. Electrostatic energies are inversely proportional to the average separation between particles, $<r>$ which is naturally proportional to $n_e^{-1/3}$. The relative importance of electrostatic energy, E_C, between a degenerate, nonrelativistic electron and an ion of charge Z, can be estimated through

$$\frac{E_C}{E_F'} \equiv \frac{Ze^2/<r>}{p_{F,e}/2m_e} \propto n_e^{-1/3} \tag{11}$$

where $E_{F,e}' = p_{F,e}^2 \propto n_e^{2/3}$ is the Fermi kinetic energy of the nonrelativistic electrons. Unlike the case of hot matter (where the mean electron kinetic energy is $\sim k_B T$), the relative importance of electrostatic corrections *decreases* with density as $n_e^{-1/3}$.

A rough estimate of the quantitative electrostatic correction can be performed by using the Wigner-Seitz approximation, which describes the lattice as neutral sphere with a central point-

like ion and an ambient uniform electron gas[3]. For a carbon or oxygen lattice, the correction to the pressure is typically of the order of a few percent. At lower densities the electron distribution deviates from uniformity, and more sophisticated approaches, namely the *Thomas-Fermi* and *Thomas-Fermi-Dirac* models, must be invoked [4, 6].

3. Neutronization Corrections to the Cold Equation of State: 10^9 **gm cm**$^{-3}$ $\rho \lesssim 4 \times 10^{11}$ **gm cm**$^{-3}$

Stable high density matter must be in chemical equilibrium to all types of reactions, including the weak interactions which drive β decay and electron capture ("inverse $\beta-$decay"):

$$n \to p + e + \bar{\nu}_e \quad , \quad p + e \to n + \nu_e , \tag{12}$$

where n and p denote a neutron and a proton, respectively, e denotes and electron and $\nu_e(\bar{\nu}_e)$ denote an electron neutrino (anti-neutrino). If the matter's composition is out of $\beta-$equilibrium, it will adjust through $\beta-$decays or electron capture. Both types of reactions change the electron per nucleon fraction, Y_e, and thus affect the EoS (Eqs. (9-10)).

In cold white dwarfs and neutron stars the weakly interacting neutrinos freely escape the system: a zero neutrino abundance implies a zero neutrino chemical potential. The condition of chemical equilibrium is then stated as:

$$\mu_n = \mu_p + \mu_e , \tag{13}$$

where μ_x denotes the chemical potential of species x. The condition of chemical equilibrium is the fundamental origin of the stable existence of neutrons in nuclei and in uniform $n - p - e$ matter. For free, single, particles the chemical potential is identical to the rest mass. The masses in MeV of the three elementary particles of Eq. (13) are $m_n = 939.6$, $m_p = 938.3$ and $m_e = 0.511$ (1 MeV is equivalent to $\sim 1.78 \times 10^{-27}$ gm). It is energetically allowed to have a *free* neutron decay in the reaction $n \to p + e + \bar{\nu}_e$ ($m_n - m_p - m_e \approx 0.8$ MeV). Indeed, the life-time of a free neutron is only about 1000 sec before it undergoes a β-decay. By contrast, in a cold, degenerate, noninteracting $n - p - e$ gas neutron decay can be "blocked": since the protons and electrons must obey the Pauli principle, the decays will be suppressed if the energy available to the newly formed electron and proton is insufficient to place them above their respective Fermi levels. At such high densities, the equilibrium state of the gas includes a finite fraction of neutrons.

In bulk matter, the electron chemical potential, which is equal to the electron Fermi energy, rises with electron number density. Hence, maintaining chemical equilibrium (Eq. 13)) may require some protons to capture electrons and covert to neutrons. In matter below the neutron drip density these conversions occur in nuclei, so their neutron fraction increases - they "neutronize". The result is a net decrease in the electron abundance (Y_e) at high densities, which lowers the pressure and "softens" the EoS.

The fact that "neutronization" becomes energetically favorable at densities below the neutron drip must be taken into account when formulating an exact EoS for this range. In matter composed

---

[3]We note that such an approximation is actually better suited for white dwarfs than for laboratory solids, where the electron distribution is much more nonuniform.

of nuclei and free electrons, β−decay is limited to relatively high densities ($\rho \geq 10^9$ gm cm^{-3}), and the exact threshold for the onset of neutronization depends on the nature of the nucleus, since the nuclear interactions must be taken into account in addition to Fermi kinetic energies. For example, the reaction $^{12}_{6}C + e \rightarrow ^{12}_{5}B$ requires the nucleus to absorb an energy of $\sim$ 14 MeV, which an electron can supply if the density of a pure carbon lattice reaches $\sim 3 \times 10^{10}$ gm cm^{-3} . The EoS of matter close to the neutron drip density is thus dependent on its chemical composition even for elements of equal Y_e, such as helium and carbon [4].

B. The Equation of State Above Neutron Drip Density: $\rho \gtrsim 4 \times 10^{11}$ gm cm^{-3}

As neutronization proceeds, the nuclei become increasingly neutron-rich. The so-called "tensor-force" component of the nuclear interactions causes like nucleons to repel one another, so that the binding energy of a neutron rich nucleus is smaller than in one where $Z/A = 0.5$. Fully equilibrated matter, reaches the last stable isotope ^{118}Kr ($Y_e \approx 0.31$) just before the density of $\rho \equiv \rho_{n-drip} \approx 4.3 \times 10^{11}$ gm cm^{-3} . At higher densities it becomes favorable for some neutrons to "drip" out of their parent nuclei. The nucleon component of the matter can no longer be confined to point-like objects and the nuclei begin to dissolve. As density is increased, a larger fraction of the nucleons exists as "free" particles, outside the nuclei. This is a gradual transition, until the matter approaches the density of atomic nuclei, where all nuclei have essentially dissolved, and the distribution of nucleons becomes uniform. The EoS above the neutron drip density must be formulated by consistently including the effects of nuclear physics, which become the governing component of the properties of matter as the density of atomic nuclei, $\rho_{nuc} \approx 2.8 \times 10^{14}$ gm/cm^3 is approached.

C. Subnuclear Densities: 4×10^{11} gm cm^{-3} $\lesssim \rho \lesssim 2.8 \times 10^{14}$ gm cm^{-3}

An analysis of cold matter in the range $\rho_{n-drip} \leq \rho \leq \rho_{nuc}$ is complicated by requiring chemical equilibrium between nucleons inside the nuclei and those that have dripped outside. One must account for the effects of the surrounding gas of free nucleons on the nuclei, as well as other effects such nuclei surface and Coulomb energies. In addition, the nuclei are expected to be very neutron rich, deviating from the $Z/A = 0.4 − 0.5$ found in terrestrial nuclei. Nonetheless, the properties of matter in this range of densities can still be derived by a natural extrapolation from ordinary nuclei, and, indeed, the EoS for such matter is believed to be well understood. The principal studies of matter (e.g., Ref. [8]) are based on the nuclear liquid-drop model, and are suitable for most applications regarding neutron star structure. For problems where a more accurate description of the neutron star inner crust is required, attention must be given to lattice effects, as the nuclei and free nucleons arrange in a distinct spatial structure (where the nuclei settle into bubbles, slabs or rods, depending on density [9]). It is expected that at $\rho \approx \frac{1}{2}\rho_{nuc}$ all nuclei will have dissolved so that the matter is completely uniform.

D. Supernuclear Densities: $\rho \gtrsim 2.8 \times 10^{14}$ gm cm^{-3}

The upper end of the high density regime is referred to as "supernuclear" where $\rho \geq \rho_{nuc}$. As matter is compressed to such densities the EoS becomes gradually dominated by the degenerate nucleons and the nucleon interactions.

It is instructive to begin by considering an ideal uniform mixture of neutrons, protons and electrons. For any given nucleon number density, n_N, solving the equilibrium composition n_n, n_p and n_e (the neutron, proton and electron number densities, respectively) requires three equations. The first is baryon number conservation,

$$n_N = n_n + n_p , \tag{14}$$

and the other two arise from imposing chemical equilibrium (Eq. 13) and charge neutrality. The condition for charge neutrality is

$$n_p = n_e . \tag{15}$$

For a noninteracting mixture of nucleons and electrons all chemical potentials are simply the Fermi energies (Eq.1)). Electrons are extremely relativistic at nuclear densities so their electron chemical potential is

$$\mu_e \approx p_{F,e}c = \hbar c (3\pi^2 Y_e \rho_B)^{1/3} \approx 100 \left(\frac{Y_e}{0.03}\right)^{1/3} \left(\frac{n_N}{n_{nuc}}\right)^{1/3} \text{MeV} , \tag{16}$$

where $n_{nuc} = 0.16$ fm^{-3} is the number density of nuclei at the saturation density (and 1 fm $= 10^{-13}$ cm). Even if the electron fraction per baryon is only a few percent, the electron chemical potential exceeds the mass difference between neutrons and protons by two orders of magnitude. The only way to maintain a finite electron fraction (which is required to balance the protons for charge neutrality) *and* satisfy chemical equilibrium is by having a significantly larger neutron than proton fraction (note that for nonrelativistic fermions $E_F \propto n^{2/3}$ and for extremely relativistic fermions $E_F \propto n^{1/3}$). Equilibrium matter at nuclear densities must be very neutron dominated, and objects composed of such matter are thus "neutron stars". For an noninteracting gas the ratio of neutrons to protons in equilibrium must be about $8:1$, which is also representative of more realistic models of supernuclear densities.

The noninteracting gas approximation is not reliable for deriving the EoS at supernuclear densities. Unlike electrostatic perturbations, nucleon-nucleon interactions are not negligible, and the interaction energies are comparable to the Fermi energies of the degenerate nucleons (electrons do not feel the strong interaction, and may still be treated as noninteracting). Modeling of the nucleon-nucleon interaction is one of the longest-standing problems in nuclear physics, still only partially solved. Profound difficulties exist due to the absence of a comprehensive theory of the interactions and the difficulty of obtaining experimental data for $\rho > \rho_{nuc}$. Further complications arise due to the fact the Fermi and interaction energies at $\rho \sim 2 - 3\rho_{nuc}$ reach a sizable fraction of the rest mass, and relativistic effects must be taken into account as well. It is not yet possible to apply quantum chromodynamics (QCD), the fundamental theory of strong interactions, to the many-body nuclear domain at $\rho \approx \rho_{nuc}$. Instead, the most useful approaches are still based on phenomenological potential formalisms, and many-body Schrödinger-like systems of equations [1].

The EoS of supernuclear matter remains to date a field of active research. Current approaches include variational methods based on deduced two and three nucleon interactions ([10], see [11] for a recent study), and relativistic mean field approximations ([12], see [13] for a review). The models are based on fitting parameters to reproduce the empirically determined properties of finite nuclei with $n = n_{nuc}$. A rough approximation of the properties of the nucleon component of supernuclear matter can be obtained through the effective, nonrelativistic model of Ref. [14],

$$\rho(n, x) = E_{gas}(n, x) + an^2 + b(n_n - n_p)^2 + cn^{\delta+1} . \tag{17}$$

The first term E_{gas} is the mass-energy density of a noninteracting gas of nucleons at density n and composition n_n, n_p. The coefficient a is negative, representing the long range attractive component of the inter-nucleon force, while c is positive, representing the short-range repulsive component. The power δ is larger than unity, so that short-range repulsion dominates at high density. The *symmetry* term includes the positive coefficient b which describes the "tensor-force" that repels like nucleons, and its contribution is therefore minimized at for symmetric nuclear matter ($n_n = n_p$). The values of a, b, c and δ are derived by requiring Eq. (17) to reproduce the assumed properties of symmetric matter at $n_N = n_{nuc}$. See Refs. [14, 15] for typical (model dependent) values of these parameters.

Finally, we note that it is quite possible that other particles, besides neutrons, protons and electrons, coexist in stable equilibrium at supernuclear matter. The most obvious example is the muon, which is a lepton similar to the electron, but has a rest mass of $m_\mu \approx 105$ MeV. The equilibrium condition for the muons will simply be $\mu_\mu = \mu_e$, so from Eq. (16) it is evident that at densities $n \gtrsim n_{nuc}$ it is energetically favorable to convert some electrons into muons through the weak interactions. At densities of $n \gtrsim 2n_{nuc}$ it possible that other exotic particles will appear, such as hyperons (baryons that are heavier than nucleons), Bose-Einstein condensates of mesons (i.e., pions or kaons), or even conversion of the nucleons into an uniform mixture of quarks (see Refs. [13, 16, 17] for recent reviews of the possible presence and roles of such particles in neutron stars).

E.   Basic Properties of High Density Matter

In Table 2 we present an EoS of cold, fully catalyzed matter ranging from normal iron at zero pressure to supernuclear densities. The EoS in the subnuclear regime is compiled from Refs. [2, 6, 8] and are "standard" for studying catalyzed high density matter. For realistic white dwarf models, which are presumably composed mostly of helium or carbon and oxygen, and never reached sufficiently high temperatures to catalyze their nuclei, a slightly different EoS must be used, based on a single species; see Ref. [4]. We also tabulate one "state-of-the-art" EoS for the supernuclear range [11]

The EoS $P(\rho)$ is plotted in Figure 1a. It is especially instructive to examine corresponding values of the adiabatic index, $\Gamma \equiv d\ln P/d\ln\rho$, plotted in Figure 1b, along with the sound speed ($c_s = \sqrt{dP/d\rho}$). Note that around $\rho \approx 10^6$ gm cm^{-3} the EoS transforms, as expected, from a nonrelativistic $\Gamma = 5/3$ polytrope to a relativistic $\Gamma = 4/3$ one as the Fermi energy of the electrons, which dominate the pressure, gradually becomes relativistic. There is a sharp drop in the adiabatic

Table 2: The equation of state [a] of cold, catalyzed high density matter[b]

ρ	n_B	P	Γ	Y	K	c_s
gm cm^{-3}	cm^{-3}	dyne cm^{-2}		dyne cm^{-2}	MeV	cm sec^{-1}
1.00E+01	6.02E+24	5.13E+11	7.03E+00	3.20E+12	7.68E-06	5.67E+05
2.00E+01	1.21E+25	2.59E+13	3.09E+00	7.32E+13	3.41E-05	1.91E+06
5.00E+01	3.01E+25	2.21E+14	2.50E+00	5.51E+14	1.03E-04	3.32E+06
1.00E+02	6.02E+25	1.13E+15	2.23E+00	2.88E+15	2.69E-04	5.37E+06
2.00E+02	1.20E+26	5.14E+15	2.14E+00	1.10E+16	5.15E-04	7.43E+06
5.00E+02	3.01E+26	3.54E+16	2.05E+00	7.27E+16	1.36E-03	1.21E+07
1.00E+03	6.02E+26	1.44E+17	1.90E+00	2.95E+17	2.75E-03	1.72E+07
2.00E+03	1.20E+27	4.91E+17	1.74E+00	8.56E+17	3.99E-03	2.07E+07
5.00E+03	3.01E+27	2.53E+18	1.82E+00	4.61E+18	8.61E-03	3.04E+07
1.00E+04	6.02E+27	9.01E+18	1.80E+00	1.75E+19	1.63E-02	4.18E+07
2.00E+04	1.20E+28	3.07E+19	1.78E+00	5.45E+19	2.54E-02	5.22E+07
5.00E+04	3.01E+28	1.51E+20	1.73E+00	2.61E+20	4.87E-02	7.22E+07
1.00E+05	6.02E+28	4.90E+20	1.69E+00	8.91E+20	8.32E-02	9.44E+07
2.00E+05	1.20E+29	1.57E+21	1.65E+00	2.59E+21	1.21E-01	1.14E+08
5.00E+05	3.01E+29	7.07E+21	1.60E+00	1.13E+22	2.11E-01	1.50E+08
1.00E+06	6.02E+29	2.16E+22	1.59E+00	3.63E+22	3.39E-01	1.90E+08
2.00E+06	1.20E+30	6.38E+22	1.57E+00	9.97E+22	4.65E-01	2.23E+08
5.00E+06	3.01E+30	2.63E+23	1.48E+00	3.90E+23	7.29E-01	2.79E+08
1.00E+07	6.02E+30	6.81E+23	1.44E+00	1.03E+24	9.64E-01	3.21E+08
2.00E+07	1.20E+31	1.88E+24	1.44E+00	2.68E+24	1.25E+00	3.66E+08
5.00E+07	3.01E+31	6.84E+24	1.40E+00	9.55E+24	1.78E+00	4.37E+08
1.00E+08	6.02E+31	1.78E+25	1.38E+00	2.57E+25	2.40E+00	5.07E+08
2.00E+08	1.20E+32	4.67E+25	1.36E+00	6.29E+25	2.94E+00	5.61E+08
5.00E+08	3.01E+32	1.53E+26	1.39E+00	2.11E+26	3.95E+00	6.50E+08
1.00E+09	6.02E+32	3.91E+26	1.17E+00	4.57E+26	4.27E+00	6.76E+08
2.00E+09	1.20E+33	8.83E+26	1.36E+00	1.19E+27	5.57E+00	7.72E+08
5.00E+09	3.01E+33	3.03E+27	1.36E+00	4.12E+27	7.71E+00	9.07E+08
1.00E+10	6.01E+33	7.24E+27	1.35E+00	1.01E+28	9.47E+00	1.01E+09
2.00E+10	1.20E+34	1.83E+28	1.24E+00	2.24E+28	1.05E+01	1.06E+09
5.00E+10	3.00E+34	5.63E+28	1.13E+00	6.37E+28	1.19E+01	1.13E+09
1.00E+11	5.99E+34	1.40E+29	1.26E+00	1.80E+29	1.69E+01	1.34E+09
2.00E+11	1.20E+35	3.13E+29	1.17E+00	3.69E+29	1.73E+01	1.36E+09
5.00E+11	2.99E+35	8.28E+29	5.60E-01	4.65E+29	8.75E+00	9.63E+08
1.00E+12	5.97E+35	1.26E+30	8.48E-01	1.05E+30	9.86E+00	1.02E+09
2.00E+12	1.19E+36	2.12E+30	7.53E-01	1.61E+30	7.60E+00	8.97E+08
5.00E+12	2.98E+36	4.79E+30	1.11E+00	5.34E+30	1.01E+01	1.03E+09
1.00E+13	5.95E+36	1.16E+31	1.44E+00	1.76E+31	1.66E+01	1.33E+09
2.00E+13	1.19E+37	3.26E+31	1.52E+00	4.94E+31	2.34E+01	1.57E+09
5.00E+13	2.97E+37	1.32E+32	1.53E+00	2.03E+32	3.84E+01	2.01E+09
1.00E+14	5.92E+37	3.93E+32	1.87E+00	8.36E+32	7.94E+01	2.88E+09
2.00E+14	1.18E+38	1.93E+33	2.75E+00	5.54E+33	2.64E+02	5.24E+09
5.00E+14	2.89E+38	1.77E+34	3.00E+00	5.54E+34	1.08E+03	1.03E+10
1.00E+15	5.50E+38	1.52E+35	2.87E+00	6.52E+35	6.68E+03	2.30E+10
2.00E+15	9.36E+38	9.20E+35	2.23E+00	3.01E+36	1.81E+04	[c]
5.00E+15	1.57E+39	4.87E+36	1.50E+00	1.44E+37	5.14E+04	[c]

[a] - shortened notation: $2.00E + 10$ is 2.00×10^{10}.

[b] - The EoS up to $\rho \sim \rho_{nuc} = 2.8 \times 10^{14}$ is based on Table 5 of Ref. [8] [© 1971. The American Astronomical Society]. The supernuclear EoS is adapted from Ref. [11].

[c] - the APR [11] EoS is not relativistic, and at extremely high densities has an unphysical superluminal (greater than light speed) speed of sound.
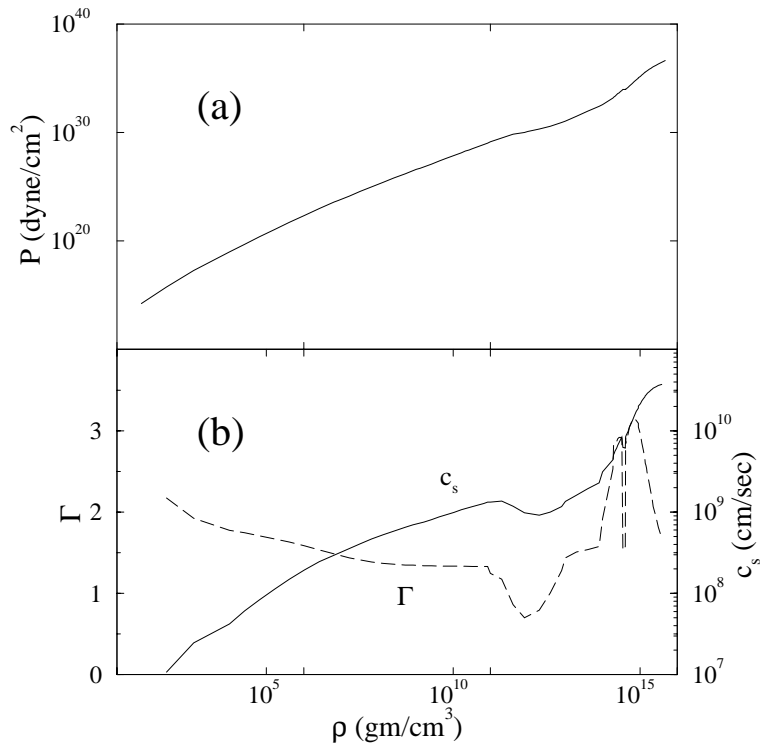
Figure 1: The equation of state of cold, catalyzed high density matter, based on Refs. [6, 8, 2, 11]: (a) the pressure density relation, (b) adiabatic index and sound speed.

index around the neutron drip density, since at first the dripped neutrons contribute to mass-density but not to pressure. Only as matter approaches nuclear densities does the nucleon pressure become important, pushing the adiabatic index back up to values in the range $2 - 3$.

Along with the EoS, we also examine some thermodynamic quantities of cold high density matter. In Table 2 we also list the adiabatic index, sound speed, bulk modulus Y, and incompressibility, K, defined as

$$Y = n\frac{dP}{dn} \quad \text{and} \quad K = 9\frac{dP}{dn} \equiv 9n\frac{d^2\rho}{dn^2} \ . \tag{18}$$

Note that the bulk modulus (which has units of pressure) is the reciprocal of the quantity usually defined as the compressibility ($\chi \equiv Y^{-1}$), while the "incompressibility" (units of energy) is more commonly used in nuclear physics applications (and is indeed measurable in nuclei). In Table 3 we list typical values of Γ, c_s, Y, K and the specific heat capacity, c_v, for condensed matter found in white dwarfs and neutron stars. For the purpose of comparison, we also give values for the sun, where the pressure roughly follows an ideal Maxwell-Boltzmann law $P \sim nk_BT$. Note how the extreme conditions of high densities leads to properties that are very different than those found for terrestrial materials. For example, the speed of sound in a neutron star is expected to be several tens of percent of the speed of light!

11

Table 3: Typical values of thermodynamic quantities in the sun, white dwarfs and neutron stars .

Object	Γ	c_s (cm sec^{-1})	Y (dyne cm^{-2})	K (MeV)	c_v ergs deg^{-1} gm^{-1}
Sun	5/3	$\sim 10^7$	$\sim 10^{12}$	$\sim 10^{-4}$	$\sim \frac{3}{2}\left(1/\mu + 1/m_p\right)k_B$
White Dwarf (C/O)	4/3	$\sim 5 \times 10^8$	$\sim 10^{24}$	~ 10	$\frac{3}{2}k_B/\mu$
Neutron Star	$2-3$	$\sim 10^{10}$	$\sim 10^{35}$	~ 200	$\sim 10^{-3}k_B/m_p$ †

† - for an ideal nonrelativistic neutron gas and a central temperature of $\sim 10^9$ °K $\rightarrow k_B T/E_F \approx 10^{-3}$.

III. White Dwarf and Neutron Star Structure

Compact objects are self-gravitating equilibria with a mass comparable to that of the sun, $1\ M_\odot \equiv 1.989 \times 10^{33}$ grams. Both white dwarfs and neutron stars are *centrally condensed* objects - most of their mass is located in a high density core, which is limited to a fraction of the volume; furthermore, the radius of the objects *decreases* with increasing mass. These traits are characteristic of a configuration supported by degenerate-fermion pressure.

A. Construction of a Self-gravitating, Equilibrium Star

The equilibrium structure of a self-gravitating object is derived from the equations of hydrostatic equilibrium. The simplest case is that of a spherical, nonrotating, static configuration, where for a given EoS all macroscopic properties are parameterized by a single parameter, for example, the central density. In the case of compact objects, the gravitational fields are strong enough that calculations must be performed in the context of general relativistic (rather than Newtonian) gravity. The fundamental equation of hydrostatic equilibrium in its general relativistic form has been derived by Tolman [19] and Oppenheimer and Volkoff [20], and is known as the "TOV" equation:

$$\frac{dP(r)}{dr} = -\frac{Gm(r)\rho(r)}{r^2}\left(1 + \frac{P(r)}{c^2\rho(r)}\right)\left(1 + \frac{4\pi r^3 P(r)}{c^2 m(r)}\right)\left(1 - \frac{2Gm(r)}{c^2 r}\right)^{-1} . \tag{19}$$

This equation simply states that at any radial distance r, the gravitational pull by the mass interior to r, $m(r)$, is balanced by the gradient of the pressure $P(r)$; $G = 6.67 \times 10^{-8}$ cm^3 gm^{-1}sec^{-2} is the gravitational constant. Note that the first term on the right hand side is the only term in the nonrelativistic case, where $P/(\rho c^2) \ll 1$ and $2Gm/(rc^2) \ll 1$. The second and third factors arise from the pressure being a form of energy density ("regeneration of pressure" effect), while the last term includes the correction due to the curvature of space in the strong gravitational field of the star.

B. Stable Configurations of High Density Matter

Given an EoS, Eq. (19) can be integrated simultaneously with the mass equation,

$$\frac{dm(r)}{dr} = 4\pi r^2 \rho(r) \ , \tag{20}$$

to determine the entire profile of the object. The actual integration is typically solved by numerical means, assuming a central density $\rho(r = 0) = \rho_c$, and integrating outward from the center until reaching the surface where $P(r) = 0$, which identifies $r = R$ as the radius of the star and $M(R)$ as its mass. We emphasize that the TOV equations provide the *gravitational* mass (or total mass-energy) of the star, which includes the effect of the gravitational binding energy, $E_{GB} \sim GM^2/R$, as well as the internal and rest mass energy of the stellar constituents. Note that in the case of neutron stars, $(GM^2/R)/(Mc^2) \sim 10 - 20\%$; indeed, the gravitational mass of a neutron star is measurably lower than the total rest mass of its constituents.
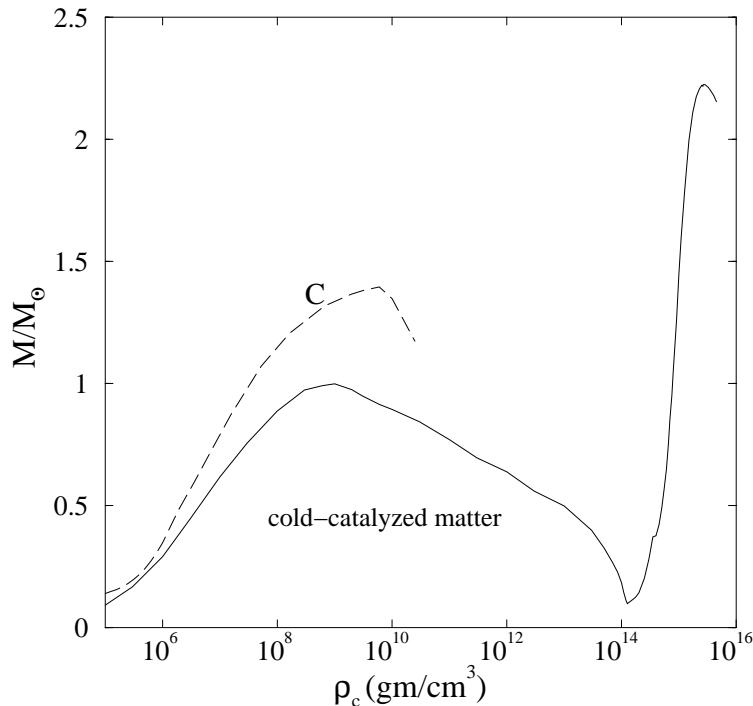

Figure 2: Mass vs. central density of a cold, carbon star [18] (dashed line) and of a star composed of cold catalyzed matter (solid line).

Varying ρ_c produces a *sequence* of models for the given EoS, yielding $M(\rho_c)$ and $R(\rho_c)$ along the sequence. The resulting sequences for stars composed of pure carbon (based on [18]) and of cold, catalyzed condensed matter (with the EoS tabulated in table 2) are both shown in Figure 2 (note that carbon dominated matter beyond the neutron drip density is unphysical and therefore omitted). The most distinct feature about the equilibrium sequences is the existence of local maxima in the
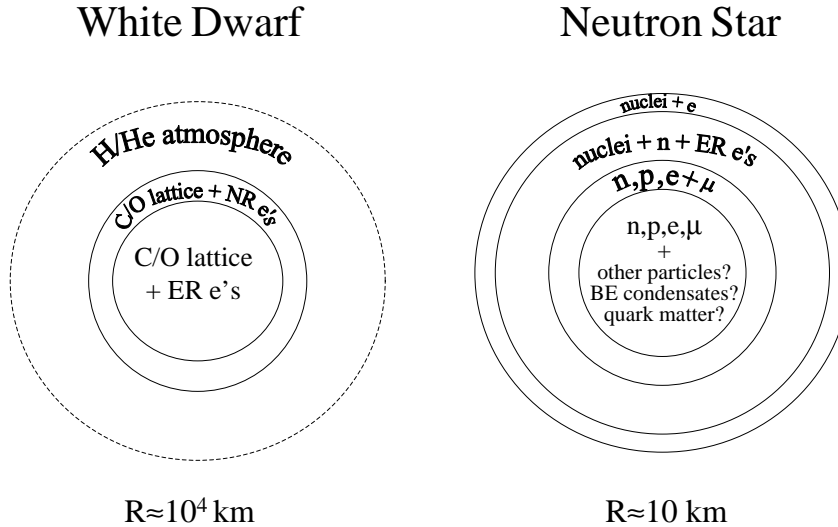
Figure 3: Schematic illustration of the structure of a typical white dwarf (left) and a neutron star (right).

$M(\rho_c)$ curves. A hydrostatic equilibrium configuration is dynamically *unstable* to catastrophic gravitational collapse if $dM/d\rho_c < 0$, since a radial perturbation would cause it to collapse on itself [1]. Therefore stable carbon white dwarfs exist only if the central density is $\rho_c \leq 6 \times 10^9$ gm cm^{-3} , while cold, catalyzed, matter has two distinct regimes of stable configurations: one with central densities below $\sim 10^{10}$ gm cm^{-3} (equivalent to white dwarfs), and one where the central density lies roughly in the range $10^{13} \leq \rho_c \leq 10^{15}$ gm cm^{-3} (neutron stars). Configurations where $\rho_c \gtrsim \rho_{n-drip}$ are unstable, and cannot be found in nature. This situation is a direct consequence of the nature of the EoS as shown in Figure 1. Quantitatively, it can be shown that a hydrostatic configuration is stable only if its mass averaged adiabatic index, $\bar{\Gamma}$, satisfies [1]

$$\bar{\Gamma} - \frac{4}{3} \gtrsim \frac{2GM}{Rc^2} \ . \tag{21}$$

It is evident therefore, that the effect of neutronization and neutron drip, which cause $\bar{\Gamma}$ to drop below $4/3$, is to separate astrophysical objects with high density matter into two distinct classes of stable configurations, which are shown schematically in Figure 3.

1. White Dwarfs

White dwarfs are composed of matter below the neutronization density. The astrophysical scenario which creates white dwarfs, i.e., quasi-static contraction of a progenitor star at the end point

of thermonuclear burning, does not allow matter to reach high enough temperatures to achieve equilibrium composition through further burning. Accordingly, the composition of white dwarfs is mostly dominated by its nuclear ashes. In the standard scenario white dwarfs are composed mostly of carbon and oxygen, but there is observational evidence that helium white dwarfs (and perhaps even iron-core white dwarfs - see below) exist as well. The pressure throughout the star is due to degenerate electrons, which are nonrelativistic in the outer layers, but are relativistic in the interior of the more massive stars with $M \sim M_\odot$.

By approximating the EoS as a Newtonian polytrope (Eq. (8)), Chandrasekar [3] derived the basic features of white dwarfs:

$$\rho_c \lesssim 10^6 \text{gm cm}^{-3} \quad \Gamma = \tfrac{5}{3}: \quad R \simeq 1.12 \times 10^9 \times \left(\frac{\rho_c}{10^6 \text{ gm cm}^{-3}}\right)^{-1/6} \left(\frac{Y_e}{0.5}\right)^{5/6} \text{ cm} \quad (22)$$

$$M \simeq 0.496 \times \left(\frac{\rho_c}{10^6 \text{ gm cm}^{-3}}\right)^{1/2} \left(\frac{Y_e}{0.5}\right)^{5} M_\odot \,,$$

$$\rho_c \gtrsim 10^6 \text{gm cm}^{-3} \quad \Gamma = \tfrac{4}{3}: \quad R \simeq 3.35 \times 10^9 \times \left(\frac{\rho_c}{10^6 \text{ gm cm}^{-3}}\right)^{-1/3} \left(\frac{Y_e}{0.5}\right)^{2/3} \text{ cm} \quad (23)$$

$$M \simeq 1.46 \times \left(\frac{Y_e}{0.5}\right)^{-2} M_\odot \,.$$

White dwarfs are expected to have radii of the order of 10^4 km - roughly the size of the Earth, or about one percent of that of the sun (which has a radius $R_\odot \approx 7 \times 10^5$ km).

As long as the EoS is approximated as a pure polytrope, so that electrostatic and neutronization corrections are ignored, helium, carbon and oxygen white dwarfs ($Y_e = 0.5$) are all identical, while an iron-dominated white dwarf is only slightly different ($Y_e \approx 0.43$). Cold, catalyzed matter, which is used for the mass sequence in Figure 2, has a significantly softer EoS (due to Y_e decreasing with increasing density), and its sequence lies, therefore, lower than those of stars composed of a single species. The most significant result in Eq. (23) is that there is no dependence of M on the central density. The mass $M_{Ch} \simeq 1.46\ M_\odot$, known as the Chandrasekar mass, is the asymptotic value a white dwarf can reach if it achieves sufficiently high density, so that its entire structure is governed by relativistic fermions (in practice this mass cannot be reached, since the outermost layer have nonrelativistic electrons). Nonrotating white dwarfs cannot have a mass exceeding M_{Ch}, and the precise limit on their mass is lower by several percent, due to neutronization at high densities (Section III.B.3.) *and* general-relativistic effects. In spite of the negligible effect on the hydrostatic equilibrium *profile* of white dwarfs, general relativity is required for a full analysis of white dwarf *stability*, since an exact $\Gamma = \tfrac{4}{3}$ star is unstable to gravitational collapse (Eq. 21).

2. Neutron Stars

Neutron stars are composed mostly of matter at nuclear densities, including a core with supernuclear densities, and is topped by a thin crust at subnuclear densities. The crust, composed of cold, catalyzed matter, may also be divided into an inner part with $\rho_{n-drip} \leq \rho \leq \rho_{nuc}$ and an outer part where $\rho \leq \rho_{n-drip}$.

Immediately after the neutron was discovered (1932) Landau modeled a neutron star as a gas of noninteracting, degenerate neutrons [21]. He found that neutron stars would have a maximum mass of about $1 M_\odot$ and a radius of several kilometers. Although this was a very crude approximation, it does suggest the correct orders of magnitude regarding the structure of these objects: a neutron star has a mass comparable to that of the sun compressed to the size of a medium city! If supported by degenerate fermion pressure, a neutron star cannot have a mass that exceeds the Chandrasekar limit by much, while its radius is inversely proportional to the mass of the pressure providing fermion. A neutron star should indeed have radius about $m_n/m_e \sim 10^3$ times smaller that of a white dwarf.
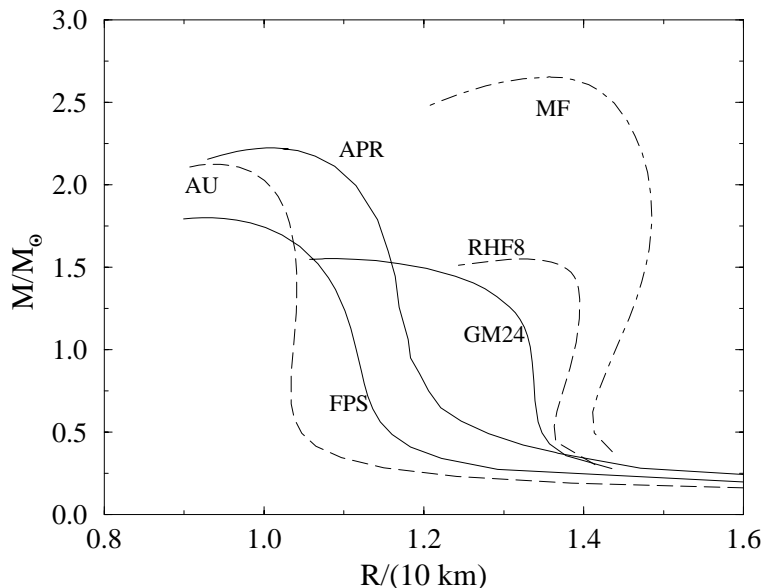

Figure 4: The mass vs. radius relation for of a nonrotating neutron star for several supernuclear equations of state: Huber et al. (RHF8, [22]), Pandharipande and Smith (MF, [23]), Glendenning (GM24, [13], page 244), Friedman and Pandharipande (FPS, [24]), Wiringa, Fiks, and Fabrocini (AU, [10]), and Akmal, Pandharipande and Ravenhall (APR, [11]).

A realistic treatment of neutron star structure requires general relativity [20], whose effects are appreciable in this case. Furthermore, quantitative estimates must be based on a realistic EoS at all densities and especially a realistic model for the supernuclear regime where particle interactions are most important. In particular, these interactions are repulsive at short distances and oppose compression, thereby stiffening the EoS in comparison to a free particle gas. Indeed, plausible equations of state predict that $M_{max}(NS) \sim 2 \ M_\odot$, ($\sim 2.2 \ M_\odot$ for Ref. [11]), whereas the star's radius will lie in the range $R \sim 10 - 15$ km. As an example, we show in Figure 4 the M vs. R relation found for a few representative equations of state of supernuclear densities. The *exact* value of $M_{max}(NS)$ depends on the assumed EoS and therefore provides an integral measure of the properties of matter at supernuclear densities [17, 25]. We also note that the existence of a maximum mass for neutron stars has important astrophysical implications, since it suggests that a larger mass cannot be sustained by cold pressure and must inevitably collapse to a black hole.

IV. Observations of Condensed Matter in White Dwarfs

Over 2000 white dwarfs have been discovered to date, based on the spectroscopic properties of observed stars [26]. While the thermal energy in white dwarfs is small compared to the Fermi energies of the electrons in the interiors, it is still sufficient to generate an observable surface luminosity for several billion years. The luminosity of a star is dependent on its radius, R, and its effective surface temperature, T_{eff}, according to

$$L = 4\pi\sigma R^2 T_{eff}^4 , \tag{24}$$

where $\sigma = 5.67 \times 10^{-5}$ erg cm^{-2} sec^{-1} deg^{-4} is the Stephan-Boltzmann constant. The luminosities of white dwarfs are typically 10^{-3} to 10^{-2} of that of the sun, $L_\odot \approx 4 \times 10^{33}$ ergs sec^{-1}, but their radii are also smaller than those of ordinary stars by a factor of ~ 100. As a result, white dwarfs have apparent surface temperature of several times 10^4 °K , unusually high in comparison with most observable stellar objects, so they do appear very "white". The existence of white dwarfs was established spectroscopically (by determining the surface temperature of sources) as early as 1910.

White dwarfs are believed to be remnants of stars with initial masses in the range $0.1 - 8~M_\odot$, which are not massive enough to complete the thermonuclear burning process all the way to iron. Mostly they are mostly composed of carbon and oxygen, but in some cases, thermonuclear burning ceased before these elements were produced, and such stars are dominated be helium.

A. Radii

Observational determination of a white dwarf radius is straightforward if its flux, F, is measured and its distance from the Earth, D, is known:

$$F(D) = \frac{L}{4\pi D^2} \quad \rightarrow \quad R^2 = \frac{FD^2}{\sigma T_{eff}^4} . \tag{25}$$

The stellar radius is derived only after the effective surface temperature is obtained spectroscopically [28]. Estimated radii of white dwarfs reside in the range of $0.007 - 0.013~R_\odot$, which is consistent with an object supported by degenerate electron pressure (Section III.B.) and thereby confirms the basic nature of white dwarfs.

B. Mass-Radius Relations

The most significant test of the nature of matter in a white dwarf is obtained by comparing observed mass-radius relations with the theoretical predictions. Once the radius of a white dwarf is determined, details of the surface emission (effects of gravitational acceleration on line emission [29] or gravitational redshift [30]) are then used to estimate the surface gravity, which scales as M/R. An independent (and usually more accurate) estimate of the mass can be obtained directly for white dwarfs in binary-star systems, through Kepler's third law [33]. Through these methods,

Table 4: Mass-radius relations of selected white dwarfs with 1σ errors. [Adapted from Provencal et al. [27], © 1998. The American Astronomical Society]

Object	Mass $(M_\odot)$	Radius $(R_\odot)$
Masses from binary motion		
Sirius B	1.000 ± 0.016	0.0084 ± 0.0002
Procyon B	0.604 ± 0.018	0.0096 ± 0.0004
40 Eri B	0.501 ± 0.011	0.0136 ± 0.0002
Masses from surface acceleration		
EG 50	0.50 ± 0.06	0.0104 ± 0.0006
GD 140	0.79 ± 0.09	0.0085 ± 0.0005
Masses from surface gravitational redshift		
CD-38 10980	0.74 ± 0.04	0.01245 ± 0.0004
W485A	0.59 ± 0.04	0.0150 ± 0.001

masses of a few white dwarfs have been estimated with reasonable accuracy, and most seem to cluster around $\sim 0.6\ M_\odot$ [31]. Some larger mass white dwarfs are also known, including the most famous Sirius B [34], with $M \approx 1\ M_\odot$. Note that these masses are smaller than M_{Ch}: it is believed that stellar evolution, and especially periods of mass loss, limit the masses of most white dwarfs to $M \leq 1\ M_\odot$, even though the EoS could sustain somewhat higher masses.

Some examples of observationally determined radii and mass for white dwarfs are presented in Table 4. Note that larger mass stars have smaller radii, as is expected (Eqs. (22-23)). It is interesting to note that for some time, there was a nonnegligible discrepancy between the observations and theory, where observed radii seemed to be $\sim 10-20\%$ smaller than estimated by theory for carbon white dwarfs [29]. Only improved estimates of distances to several white dwarfs with the *Hipparcos* satellite, and better modeling of white dwarf atmospheres [35] have allowed this discrepancy to be mostly resolved [27]. A comparison of current observed mass-radii determinations with theoretical curves is presented in Figure 5, and in general, the fit is indeed very good: these new results seem to confirm that the composition of most white dwarfs is indeed dominated by medium weight elements (carbon and oxygen). However, they also imply that a small minority of white dwarfs do have relatively small radii, and may therefore contain iron cores, which presents an intriguing puzzle from the point of view of stellar evolution.

Figure 5: The mass-radius relation for white dwarfs. Solid lines labeled He, C, Mg, and Fe denote the zero-temperature mass-radius relation for a star composed of each element of Ref. [18]. Models of white dwarfs with a hydrogen atmosphere [35] are for an effective atmosphere temperature of 30,000°K (dotted line) and 15,000°K and 8000 °K (dashed lines). Estimates for observed white dwarfs are shown with a 1σ error. [From Provencal et al. [27], © 1998. The American Astronomical Society]
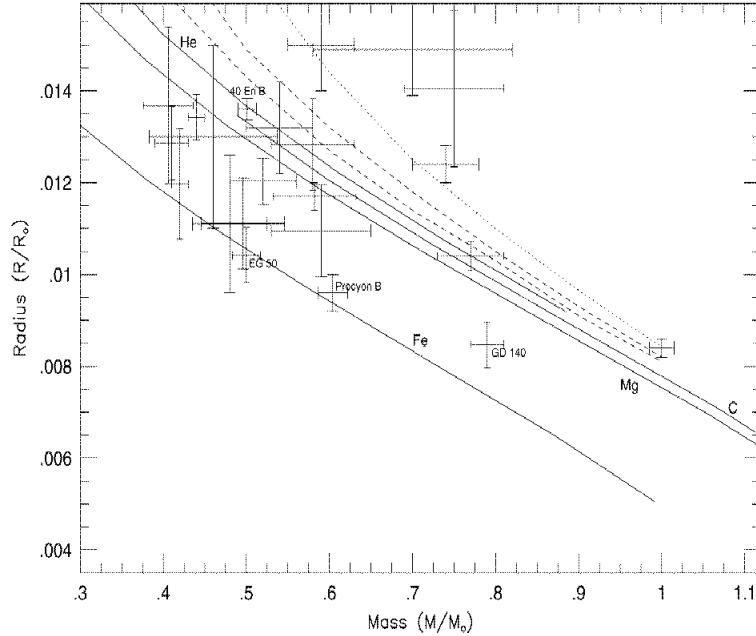
V.   Observations of Condensed Matter in Neutron Stars

Neutron stars are often identified observationally as very accurately pulsating sources, where the pulsation is attributed to the star's rotation. The period of pulsation limits the size of the source to no more than a few tens of kilometers, thus indicating the presence of a very compact object. Since the first discovery in 1967, close to 800 pulsars have been identified, over 700 of those in radio waves [36]. About thirty X-ray pulsars have also been observed, and a smaller number of nonpulsating X-ray sources of various types are also most likely to contain a neutron star [37].

Theory suggests that neutron stars are formed when a massive star is disrupted in a "supernova" explosion. As the massive star evolves, matter in its core undergoes thermonuclear burning all the way to iron, which is the most tightly bound nucleus and therefore cannot burn further. When the iron core is massive enough it collapses under its own weight, until the collapse is halted when nuclear densities are reached. Most of the gravitational binding energy is released in the form of neutrinos, but some is transformed into an outgoing shock wave that expels the star's envelope and leaves behind the newly formed neutron star. Indeed, several dozen young neutron stars have been found in sites of past supernovae, confirming this scenario.

A. Neutron Star Masses

The masses of over twenty neutron stars have been determined observationally through their gravitational pull on a binary companion star. Within the errors of measurement, the masses of these stars appear to cluster in a narrow range of 1.35 ± 0.1 $M_{\odot}$ [38]. This is especially true of the masses of neutron stars in the five known binary-pulsar systems (where the companion object is also a neutron star), listed in Table 5, where mass determinations are most accurate. In particular, the Hulse-Taylor binary pulsar 1913+16 (the galactic coordinates of its location) has been very accurately determined to have $M_{1913+16} = 1.4411 \pm 0007$ $M_{\odot}$. Clearly, a high density EoS must satisfy $M_{max} \geq 1.44$ $M_{\odot}$ to be consistent with this observation.

Table 5: Mass determinations with errors of neutron stars in known binary pulsar systems. [Adapted from Thorsett and Chakrabarty [38], © 1999. The American Astronomical Society].

Star	Median mass mass ($M_{\odot}$)	68% central limits	95% central limits
J1518+4904 pulsar	1.56	$+0.13/-0.44$	
J1518+4904 companion	1.05	$+0.45/-0.11$	
B1534+12 pulsar	1.339	± 0.003	± 0.006
B1534+12 companion	1.339	± 0.003	± 0.006
B1913+16 pulsar	1.4411	± 0.00035	± 0.0007
B1913+16 companion	1.3874	± 0.00035	± 0.0007
B2127+11C pulsar	1.349	± 0.040	± 0.080
B2127+11C companion	1.363	± 0.040	± 0.080
B2303+46 pulsar	1.30	$+0.13/-0.46$	$+0.18/-1.08$
B2303+46 companion	1.34	$+0.47/-0.13$	$+1.08/-0.15$

This mass limit does not impose a serious constraint on realistic models for the supernuclear EoS and is satisfied by all but the softest equations. There has been much debate whether the narrow range of observed neutron star masses is evidence for the maximum mass being rather low ($M_{max}(NS) \approx 1.5$ $M_{\odot}$) [39], or whether it is due to astrophysical effects, which could restrict the range of masses of observable stars. Recently, there is growing evidence that heavier neutron stars exist: the Vela pulsar is now estimated to have a mass of ~ 1.9 $M_{\odot}$ [40], and the oscillations observed in some galactic X-ray sources seem to indicate that they include neutron stars with masses larger than 2 $M_{\odot}$ [41]. If these estimates are confirmed with improved observations in the future, they will provide a much more stringent test that would be consistent only with the stiffer models for the supernuclear EoS.

B. Radii

The mass and radius relation of a nonrotating neutron star is uniquely defined for any given EoS through the solution of the TOV equations (Figure 4). However, to date, observational methods for

estimating neutron star radii lack the accuracy required to critically differentiate between realistic equations of state. Hopefully, data from a new generation of X-ray satellites will provide substantial constraints on the compactness (M/R) of neutron stars (either through their thermal emission [42] or from emission of material accreting upon them [43]).

C.   Rotation periods

The observed pulsation period of a neutron star is attributed to rotation. Most measured periods are in the range $0.25 - 1$ sec, but a subclass of *millisecond* pulsars are also known to exist. The fastest spinning neutron star observed to date has a period of $P = 1.56$ msec (so that it spins faster than an egg-beater!).

Rotation provides an additional centrifugal barrier which assists the internal pressure in supporting the gravitational load. The resulting configuration is then dependent on both central density and rotation period, and must be solved self-consistently including the effects of general relativity. The maximum mass a given equation of state can support increases with respect to the static (TOV) value as the star is allowed to rotate faster [44]. There must exist a lower limit on the rotation *period* (upper limit on the rotation *rate*), since too rapid rotation would cause the star to shed mass at the equator. The general trend is that a softer EoS predicts a smaller lower limit on the rotation period, since a more compact star is more tightly bound gravitationally and so is better suited to resist the centrifugal force. At present, the limit of ~ 1.56 msec is not very restrictive, and is consistent with basically all realistic models of high density matter. Discovery of a sub-millisecond $(P \gtrsim 0.5$ msec) pulsar would allow to distinguish more directly between competing supernuclear equations of state [1, 45, 46].

D.   Pulsar Glitches

Pulsar periods are observed to increase gradually with time, implying that rotational energy of the star is being lost (primarily by electromagnetic dipole radiation). However, several pulsars have been observed to undergo sudden *decreases* in the rotation period, which are believed to originate from the transfer of angular momentum between different parts of the star. The current leading model [47, 48] suggests that the source of excess angular momentum is the inner curst, and thus the magnitude of glitch phenomena can be used to set a lower limit on the fraction of the total moment of inertia the inner crust must carry. Recent results [49] suggest the crust of the Vela pulsar must carry at least 1.4% of the total moment of inertia of the star, which is sufficient to rule out equations of state which are very soft in the range $1 \leq \rho/\rho_{nuc} \leq 2$. Possible progress in theoretical modeling of glitch phenomena could provide further limits on the properties of high density matter near the nuclear saturation density.

VI.   Thermal Properties of Matter in White Dwarfs and Neutron Stars

Fermions in both white dwarfs and neutron stars are expected to have degenerate energies which are much larger than their thermal energies. However, compact objects do have finite temperatures that are a relic of their progenitors. Since degenerate matter has very long scattering lengths for individual particles, the cores of both white dwarfs and neutron stars are expected to be excellent thermal conductors, and practically isothermal.

Finite temperature effects on the properties of condensed matter in compact objects has become a very active theoretical and observational field in recent years, especially in the case of white dwarfs. A finite temperature leads to cooling through thermal emission processes which are potentially observable. Examining the cooling history (i.e., temperature vs. age) of compact objects thus provides empirical evidence regarding the thermal properties of high density matter. Here we can only briefly mention some of the topics of current interest.

A.   Thermal Effects in White Dwarf Structure

The region most affected by a finite temperature is the low density outer-layers of a white dwarf, which may include a thin atmosphere composed of helium and possibly also hydrogen. For lower densities the electrons are not degenerate and a surface temperature of 10^4 °K will severely alter the equation of state, especially in the regime where electrostatic corrections are important. Modern equations of state for a hydrogen/helium atmosphere [50] have been incorporated in several studies of white dwarf structure (see [51] for helium stars, [35] for carbon-oxygen, and [52] for a recent compilation of various compositions). The thermal pressure in the outer layers is generally found to be very effective in inflating the stellar radius. As seen from Figure 5, a surface temperature of $T_{eff} = 10^4$ °K increases the radius by a factor of two [35, 52] with respect to the cold [18] models.

There has been a recent revival of studies of white dwarf thermal evolution, and its dependence on the properties of matter at the relevant high densities. We briefly review here the two main aspects of these studies, namely cooling and pulsations.

1.   White Dwarf Cooling

The basic theory of white dwarf cooling was established by Mestel in 1952 [53]. The heat is originally stored in the nondegenerate ion-lattice, and the dominant cooling mechanism is photon diffusion to the surface from the isothermal core through the nondegenerate outer layers. The simplest results are based on Kramer's approximation for the photon opacities in the nondegenerate regime:

$$\kappa = \kappa_0 \rho T^{-3.5} , \tag{26}$$

where κ is the mean opacity (in $cm^2 gm^{-1}$) and $\kappa_0 = 4.34 \times 10^{24} Z(1+X_H)$ $cm^2 gm^{-1}$ is a composition dependent constant, X_H and Z being the mass-fraction of hydrogen and heavy (not hydrogen or

helium) elements, respectively. The luminosity through the outer layers, $L(r)$, is dependent on the temperature gradient according to the radiative diffusion equation

$$L(r) = -4\pi r^2 \frac{c}{3\kappa\rho}\frac{d}{dr}(aT^4) \qquad (27)$$

(where $a = 7.7565 \times 10^{-15}$ erg deg^{-4} is the radiation constant). Combining the above thermal temperature gradient with the pressure gradient required for hydrostatic stability (Eq. (19), see [1]), one finds that the surface luminosity satisfies

$$L = 5.7 \times 10^6 \mu Y_e^2 \frac{1}{Z(1+X)}\left(\frac{M}{M_\odot}\right)T_c^{3.5} , \qquad (28)$$

where μ is the mean molecular weight in the nondegenerate atmosphere and T_c is the core temperature in the star. For typical white dwarfs ($M \sim 1\ M_\odot$) with no hydrogen in the atmosphere, $X = 0$, $Z \approx 0.1$, $\mu = 1.4$, $Y_e = 0.5$, an observed luminosity in the range 10^{-5}–$10^{-2}\ L_\odot$ corresponds to a central temperature of $T_c \sim 10^6 - 10^7$ °K .

The key elements of Eq. (28) are that the surface luminosity (which is observable) is clearly related to the mass of the star, the composition and the internal temperature. If the mass is also determined separately (as discussed above), luminosity can then provide a direct test of the star's thermal and composition profiles. Furthermore, the age of the white dwarf can also be estimated based on its cooling time scale, which is dependent on the luminosity function (Eq. 28), the stellar mass and the specific heat capacity of a white dwarf material. The latter (in ergs deg^{-1} gm^{-1}) if roughly that of the ion lattice,

$$c_v(\text{ions}) = 2\frac{3}{2}\frac{k_B}{\mu} , \qquad (29)$$

where the factor of 2 comes from the three degrees of collective vibration and rotation, in addition to the three single ion degrees of motion. Due to their degeneracy, the specific heat capacity of the electrons is suppressed by a factor of $\sim k_B T/E_F$ [54], which for a density of 10^8 gm cm^{-3} and an internal temperature of $\sim 10^7$ °K is 10^{-3}.

While models which include more detailed microphysics do reproduce the general results of the Mestel model (see, for example, in Refs. [1, 32, 55, 56]), accurate work that is compatible with the quality of current observations must include several important perturbations. Most notably, accurate low temperature opacities, semidegenerate electron thermal conductivity and pressure-induced ionization must be accounted for in modeling the white dwarf atmosphere. Crystallization of the ion gas may also have a significant effect on the thermal history of the star, both as a transient source of (latent) heat and by effectively reducing the heat capacity. In particular, below the *Debye temperature*, $\Theta_D \simeq 4 \times 10^3 \rho^{1/2}$ °K , the specific heat capacity becomes temperature dependent [1],

$$c_v = \frac{12\pi^4}{5}k_B\left(\frac{T}{\Theta_D}\right)^3 . \qquad (30)$$

The specific effects of the finite temperature on the thermodynamic properties of matter in white dwarf atmosphere are most notable through studies of pulsations (see below).

It is noteworthy that for several years there seemed to be a paucity of low-luminosity (and therefore, old) observed white dwarfs, which posed a nontrivial puzzle in terms of models for the

stellar evolution. Only rather recently it was realized [57] that the properties of the finite temperature atmospheres would make old white dwarfs dimmer than previously anticipated (especially if their atmosphere included only a helium layer and no hydrogen).

2. Pulsation of White Dwarfs

The basic theory of stellar pulsation is reviewed in detail by Sarbani Basu in this volume. We note that studies of pulsations in general allow one to estimate the sound speed profile of the star, its temperature gradient, and even the mean molecular weight in its core. It has been well established [58] that stellar pulsation provides an effective probe for the properties of matter in a star. Commonly referred to as "astroseismology", this field is rapidly emerging due significant advances in observational instrumentation and theoretical modeling.

White dwarfs, like many other stars, may undergo stable pulsations which leave a detectable imprint on the time dependence of the star's luminosity [59, 60]. Since pulsations tend to damp over time, they are most easily observable in younger, and therefore hotter, white dwarfs. Modeling observed pulsations of young white dwarfs is particularly important for probing the EoS of semidegenerate matter [61, 62]. With the aid of theoretical models, studies of white dwarfs pulsations have been used for independently restricting the mass-radius relationships and dimensions of the hydrogen envelope [60, 63], and in general seems to hold much potential for future studies of the details of white dwarf physics. For example, some pulsation modes are theoretically predicted to be more sensitive to the extent of crystallization of the atmosphere material. Recent analysis of the periods and relative magnitudes various pulsation modes in the white dwarf BPM 37093 [62] helps determine the extent of crystallization in the atmosphere (about 50% in mass), which compares favorably with theory. In another recent example [64], it is possible to identify, for the first time, the contraction rate of the pre-white dwarf star PG 1159-035, by measuring the secular changes over time of the periods of various modes.

B. Thermal Effects in Neutron Star Structure

Although finite temperature effects are practically negligible when considering the overall structure of evolved neutron stars, they are important in assessing their thermal history and as probes of matter in the interior of these objects. Some thermal effects on structure do exist in newly-born neutron stars (often called "proto-neutron star").

1. Proto-Neutron Stars

Neutron stars are born in supernovae with initial internal temperatures of several times 10^{11} °K and initial entropies of $\sim 2k_B$ per nucleon (k_B is the Boltzmann constant). These values are large enough to impose nontrivial effects on the composition and structure of the neutron star compared to the $T = 0$ case [16]. At such high temperatures the matter is *not* transparent to the thermal neutrinos

[1, 65], and the proto-neutron star must cool through neutrino diffusion to the surface, which occurs over a time scale of several seconds (much longer than a dynamical time of milliseconds) [66]. This fundamental prediction was dramatically confirmed by the observed neutrino pulse from the supernova 1987A (the closest supernova observed from the Earth in 400 years), which lasted for ~ 12 seconds. (see [67] for a review). Further studies of the properties of high temperature, supernuclear-density matter are required to model this brief early cooling epoch and its possible observational signatures [68].

2.   Cooling of Neutron Stars

After the initial rapid cooling stage which lasts several days, a neutron star settles on a slower cooling curve [1, 69]. Once neutrinos escape the system freely, they must be continuously produced in order to fuel the emission process. Subsequent neutrinos are mostly produced by the so-called URCA (β and inverse β decays as in Eq. (12)) and other processes. The isothermal core at this stage is expected to have temperature of several times 10^8 °K , while at the surface the temperature is down to several times 10^6 °K - which provides for continuous surface thermal luminosity in soft X-rays. This soft X-ray luminosity is much more difficult to detect than the optical ultraviolet luminosity white dwarfs. Current observations are generally limited to young (age $\lesssim 10^6$ yrs) neutron stars, where the main cooling mechanism is still the neutrino emission from the core. An important consequence of this situation is that estimates of thermal emission from neutron stars serve as a probe of the properties of matter in the core [70].

Over 20 compact, isolated soft X-ray sources observed with X-ray imaging telescopes have been identified as neutron stars [71]. In most cases the source is either too faint to allow for a spectroscopic determination of the surface temperature, or the emission is dominated by other phenomena (most likely magnetospheric emission). However, in a hand-full of cases surface thermal emission has been strong enough to be detected and the surface temperature has been deduced to within a factor of two [71]. The measurements are still not accurate enough to determine whether the observed layer is the actual surface or a possible hydrogen atmosphere, which would have different emission properties, but they are sufficient to place some constraints on the rates of neutrino emitting processes in the core [72].

Perhaps the most notable conclusion to date of observed neutron star cooling rates is that they support the theoretical prediction that the nucleons in the core couple to a *superfluid* state. Theoretical models suggest that the strong interactions will pair the neutrons in the core in a $^3P_1$ superfluid and the protons to a $^1S_0$ superconductor with critical temperatures of the order of 10^9 °K [73]. Neutrino emitting processes, such as β-decays must break a coupled Cooper pair before its constituents can participate in the decay. The main effect of nucleon superfluidity is therefore damping the efficiency of neutrino emission from the core (there is also a secondary effect due to the modulation of the heat capacity, which first increases discontinuously as the star cools to the critical temperature, and then decreases exponentially at lower temperatures). Observed neutron star surface temperatures are apparently too high to be consistent with the cooling rates predicted for normal core, but they agree with the suppressed cooling rates when the nucleons couple to a superfluid state [74, 75]. Further progress in analyses of the matter in the interiors of neutron stars

is expected through measurements by NASA's recently launched Chandra X-ray satellite.

VII. Concluding Remarks

The theoretical and observational study of compact objects remains one of the most exciting fields in modern astronomy. In essence, this research is also an exploration of the properties of condensed matter at extreme densities. Predictions regarding the properties of white dwarfs and neutron stars serve to test our understanding of matter at these high densities, while theories of high density matter serve as a basis for interpreting observational results regarding these objects. Most exciting, these objects bring together all four of the fundamental forces of nature and probe regimes not accessible in the terrestrial laboratory. They provide the most numerous and accessible sample of objects where relativistic gravitation - general relativity - plays a role in determining their physical properties.

In this review we have described the tight interconnection between the microscopic (local) properties of condensed matter at high densities and the macroscopic (global) properties of white dwarfs and neutron stars. While the fundamental principles of cold, high density matter are believed to be well understood, and are generally consistent with observations, key questions still remain, and new observations may give rise to new puzzles. The current boom in capabilities of Earth-bound telescopes and satellite instrumentation promises that many more puzzles - and hopefully, answers - are in store regarding the nature of cosmic matter at high densities.

References

[1] Shapiro, S. L., and Teukolsky, S. A. (1983). *"Black Holes, White Dwarfs and Neutron Stars"*. Wiley, New York, NY.

[2] Baym, G., Pethick, C. J., and Sutherland, P. (1971). The ground state of matter at high densities: Equation of state and stellar models. *Astrophys. J.*, **170**, 299.

[3] Chandrasekar, S. (1931). The density of white dwarf stars. *Phil. Mag.* **11**, 592; The maximum mass of ideal white dwarfs. *Astrophys. J.***74**, 81.

[4] Salpeter, E. E. (1961). Energy and pressure of zero temperature plasma. *Astrophys. J.*, **134**, 669.

[5] Dirac, P. .A. M. (1926). On the theory of quantum mechanics. *Proc. Roy. Soc. London Ser. A*, **112**, 661.

[6] Feynman, R. P., Metropolis, N., and Teller, E. (1949). Equations of state of elements based on the generalized Fermi-Thomas Theory. *Phys. Rev.*, **75**, 1561.

[7] Harrison, B. K., and Wheeler, J. A. (1958). See *in* Harrison, B. K., Thorne, K. S., and Wheeler, J. A. (1965). Gravitation theory and gravitational collapse. University of Chicago Press, Chicago.

[8] Baym, G., Bethe, H. A., and Pethick, C. J. (1971). Neutron star matter. *Nucl. Phys. A*, **175**, 225.

[9] Ravenhall, D. G., and Pethick, C. J. (1995). Matter at large neutron excess and the physics of neutron-star crusts. *Ann. Rev Nuc. Pat. Sci.*, **45**, 429.

[10] Wiringa, R. B., Fiks, V., and Fabrocini, A. (1988). Equation of state for dense nuclear matter. *Phys. Rev.* **C**, **38**, 1010

[11] Akmal, A., Pandharipande, V. R. and Ravenhall, D. G. (1998). The equation of state for nucleon matter and neutron star structure. *Phys. Rev.* **C58**, 1804.

[12] Serot, B. D., and Walecka, J. D. (1979). Properties of finite nuclei in a relativistic quantum field theory. *Phys. Lett. B*, **87**, 172.

[13] Glendenning, N. K (1996). "*Compact Stars*", Springer, New York, NY.

[14] Lattimer, J. M., and Swesty, D. F. (1991). An effective equation of state for hot dense matter. *Nucl. Phys. A*, 535, 331

[15] Balberg, S., and Gal, A. (1997). An effective equation of state for dense matter with strangeness. *Nucl. Phys. A*, **625**, 435.

[16] Prakash, M. et al. (1997). Composition and structure of proto-neutron stars. *Phys. Rep.*, **280**, 1.

[17] Balberg, S, Lichtenstadt, I., and Cook, G. B. (1999). Roles of hyperons in neutron stars. *Astrophys. J. Supp.*, **121**, 515.

[18] Hamada, T., and Salpeter, E. E. (1961). Models for zero-temperature stars, *Astrophys. J.*, **134**, 683.

[19] Tolman, R. C. (1939). Static solutions of Einstein's filed equations for spheres of fluids. *Phys. Rev.*, **55**, 364.

[20] Oppenheimer, J. R., and Volkoff, G. M. (1939). On massive neutron cores. *Phys. Rev.*, **55**, 374.

[21] Landau, L. D. (1932). On the theory of stars. *Phys. Z. Sowjwtunion*, **1**, 285.

[22] Huber, H., Weber, F., Weigel, M. K., and Schaab, Ch. (1998). Neutron star properties with relativistic equations of state. *Int. J. Mod. Phys. E*, **7**, 301.

[23] Pandharipande, V. R., and Smith, R. A. (1975). Nuclear matter calculations with mean stellar fields. *Phys. Lett. B*, **59**, 15.

[24] Friedman B., and Pandharipande, V. R. (1981). Hot and cold, nuclear and neutron matter. *Nucl. Phys. A*, **361**, 502.

[25] Pandharipande, V. R., Pines, D., and Smith, R. A. (1976). Neutron star structure: theory, observation and speculation. *Astrophys. J.*, **208**, 550.

[26] McCook, G. P., Sion, E. M. (1999). A catalog of spectroscopically identified white dwarfs. *Astrophys. J. Supp.*, **121**, 1.

[27] Provencal, J. L., Shpiman, H. L., Høg, E., and Thejll, P. (1998). Testing the white dwarf mass-radius relation with *HIPPARCOS. Astrophys. J.*, **494**, 759.

[28] Shipman, H. L. (1979). Masses and Radii of white dwarfs III. Results for 110 hydrogen-rich and 28 Helium-rich stars. *Astrophys. J.*, **228**, 240.

[29] Schmidt, H. (1996). The empirical white dwarf mass-radius relation and its possible improvement by HIPPARCOS. *Astron. Astrophys.*, **311**, 852.

[30] Shapiro, S. L., and Teukolsky, S. A. (1976). On the maximum gravitational redshift of white dwarfs. *Astrophys. J.*, **203**, 697.

[31] Weidermann, V. (1990) Masses and evolutionary status of white dwarfs and their progenitors. *Ann. Rev Astron. Astrophys.*, **28**, 103.

[32] D'Antona, F., and Mazzitelli, I. (1990). Cooling of white Dwarfs. *Ann. Rev Astron. Astrophys.*, **28**, 139.

[33] Greenstein J, L. (1986). White dwarfs in wide binaries. I - Physical properties. II - Double degenerates and composites. *Astron. J.*, 92, 859.

[34] Gatewood, G. D., and Gatewood, C. V. (1978). A study of Sirius. *Astrophys. J.*, **225**, 191.

[35] Wood, M. A. (1995). Theoretical white dwarf luminosity functions: DA models. *In* "Proc. 9th European Workshop on White Dwarfs" (D. Koster and K. Werner, Eds.), pp. 41. Springer, Berlin.

[36] Taylor, J. H., Manchester, R. N., and Lyne, A. G. (1993). Catalog of 558 pulsars. *Astrophys. J. Supp.*, **88**, 529. See the Princeton Pulsar-Group website for an updated catalog, http://www.pulsar.princeton.edu.

[37] *X-Ray Binaries*, W. H. G. Lewin, J. van Paraijs and E. P. J. van den Heuvel, Eds. (1995). Cambridge University Press, Cambridge.

[38] Thorsett, S. E., and Chakrabarty, D. (1999). Neutron star mass measurements. I. Radio pulsars. *Astrophys. J.*, **512**, 288.

[39] Bethe, H. E., and Brown, G. E. (1995) Observational constraints on the maximum neutron star mass. *Astrophys. J. Lett.*, 445, L29.

[40] van Kerkwijk, M. H. (2000) Neutron Star Mass Determinations. *To appear in* "Proc. ESO Workshop on Black Holes in Binaries and Galactic Nuclei", (L. Kaper, E. P. J. van den Heuvel, and P. A. Woudt, Eds.). Springer-Verlag, Berlin (available on the Los-Alamos pre-print server, astro-ph/0001077).

[41] van der Klis, M. (1998) KlioHertz quasi-periodic oscillations in low mass X-ray binaries. *In* "The Many Faces of Neutron Stars", NATO ASI series (R. Buccheri, J. van Paradijs and M. A. Alpar, Eds.), pp. 337. Kluwer, Dordrecht.

[42] Ögelman, H. (1995). X-ray observations of cooling neutron stars. *In* "The Lives of the Neutron Stars" (M. A. Alpar, Ü. Kizilogu and J. van Paradijs, Eds.), pp. 101. Dordechet, Kluwer.

[43] Miller, M. C., and Lamb, F. K. (1998). Bounds on the compactness of neutron stars from brightness oscillations during X-Ray bursts. *Astrophys. J. Lett.*, **499**, L37.

[44] Cook, G. B., Shapiro, S. L., and Teukolsky, S. A. (1994). Rapidly rotating neutron stars in general relativity: Realistic equations of state *Astrophys. J.*, **424**, 823.

[45] Shapiro, S. L., Teukolsky, S. A., and Wasserman I. (1983). Implications of the millisecond pulsar for neutron star models. *Astrophys. J.*, **272**, 702.

[46] Lattimer, J. M., Prakash, M., Masak, D., and Yahil, A. (1990). Rapidly rotating pulsars and the equation of state. *Astrophys. J.*, **355**, 241

[47] Pines, D., and Alpar, M. A. (1985). Superfluidity in neutron stars. *Nature*, 316, 27.

[48] Alpar, M. A., Chau, H. F., Cheng, K. S.,and Pines, D. (1993). Postglitch relaxation of the VELA pulsar after its first eight large glitches - A reevaluation with the vortex creep model. *Astrophys. J.*, 409, 345.

[49] Link, B., Epstein, R. I., and Lattimer, J. M. (1999). Pulsar constraints on neutron star structure and equation of state. *Phys. Rev. Lett.*, **83**, 3362.

[50] Saumon, D., Chabrier, G., and van Horn, H. M. (1995). An equation of state for low-mass stars and giant planets. *Astrophys. J. Supp.*, **99**, 713.

[51] Hansen, B. M. S., and Sterl Phinney, E. (1998). Stellar forensics. I - Cooling curves. *Mon. Not. Roy. Astron. Soc.*, **294**, 557.

[52] Panei, J. L., Althaus, L. G., and Benvenuto, O. G. (2000). Mass-radius relations for white dwarfs of different internal compositions. *Astron. Astrophys.*, **353**, 970.

[53] Mestel, L. (1952). On the theory of white dwarfs stars I. The energy sources of white dwarfs. *Mon. Not. Roy. Astron. Soc.*, **112**, 583.

[54] Pathria, R. K. (1972). *Statistical Mechanics*. Pergamon Press, Oxford.

[55] Iben, I., Jr., and Tutukov, A. V. (1984). Cooling of low-mass carbon-oxygen dwarfs from the planetary nucleus stage through the crystallization stage. *Astrophys. J.*, **282**, 615.

[56] Hansen, B. M. S. (1999). Cooling models for old white dwarfs. *Astrophys. J.*, **520**, 680.

[57] Hansen, B. M. S. (1998). Old and blue white-dwarf stars as a detectable source of microlensing events. *Nature*, **394**, 860.

[58] Cox, J. P. (1980). *Theory of Stellar Pulsation*. Princeton University Press, Princeton, NJ.

[59] Bradley, P. A., Winget, D. E., and Wood, M. A. (1993). The potential for astroseismology of DB white dwarf stars. *Astrophys. J.*, **406**, 661.

[60] Bradley, P. A., and Winget, D. E. (1991). Astroseismology of white dwarf stars. I - Adiabatic results. *Astrophys. J. Supp.*, **75**, 463.

[61] Bradley, P. A., Winget, D. E., and Wood, M. A. (1993) Maximum rates of period change for DA white dwarf models with carbon and oxygen cores. *Astrophys. J. Lett.*, **391**, 33.

[62] Montgomery, M. H., and Winget, D. E. (1999). The effect of crystallization on the pulsations of white dwarf stars. *Astrophys. J.*, **526**, 976.

[63] Goldreich, P., and Wu, Y. (1999). Gravity modes in ZZ Ceti stars. I. Quasi-adiabatic analysis of over-stability. *Astrophys. J.*, **511**, 904; Gravity modes in ZZ Ceti stars. II. eigenvalues and eigenfunctions. *Astrophys. J.*, **519**, 783.

[64] Costa, J. E. S., Kepler, S. O., and Winget, D. E. (1999). Direct measurement of a secular pulsation period change in the pulsating hot pre-white dwarf PG 1159-035. *Astrophys. J.*, **522**, 973.

[65] Reddy, S., and Prakash, M. (1997). Neutrino scattering in a newly born neutron star. *Astrophys. J.*, **423**, 689.

[66] Burrows, A., and Lattimer, J. M. (1986). The birth of neutron stars,. *Astrophys. J.*, **307**, 178.

[67] Bethe, H. E. (1990). Supernovae. *Rev. Mod. Phys*, **62**, 801.

[68] Pons, J. A., Reddy, S., Prakash, M., Lattimer, J. M., and Miralles, J. A. (1999). Evolution of Proto-Neutron Stars. *Astrophys. J.*, **513**, 780.

[69] Pethick, C. J. (1992). Cooling of neutron stars. *Rev. Mod. Phys*, **64**, 1133.

[70] Schaab, Ch., Weber, F., Weigel M. K., and Glendenning, N. K. (1996). Thermal evolution of compact stars. *Nucl. Phys. A*, 605, 531.

[71] Schaab, Ch., Weber, F., and Weigel, M. K. (1998). Neutron superfluidity in strongly magnetic interiors of neutron stars and its effect on thermal evolution. *Astron. Astrophys.*, **335**, 596.

[72] Page D. (1998). Thermal evolution of isolated neutron stars. *In* "The Many Faces of Neutron Stars", NATO ASI series (R. Buccheri, J. van Paradijs and M. A. Alpar, Eds.), pp. 539. Kluwer, Dordrecht.

[73] Takatsuka, T. and Tamagaki, R. (1993). Superfluidity in neutron star matter and symmetrical nuclear matter. *Prog. Theo. Phys. Suppl.*, **112**, 27.

[74] Schaab, Ch., Voskresensky, D., Sedrakian, A. D.,Weber, F., and Weigel, M. K. (1997). Impact of medium effects on the cooling of nonsuperfluid and superfluid neutron stars. *Astron. Astrophys.*, 321, 591.

[75] Schaab, Ch., Balberg, S., and Schaffner-Bielich, J. (1998). Implications of hyperon superfluidty for neutron star cooling. *Astrophys. J. Lett.*, 504, L99.